

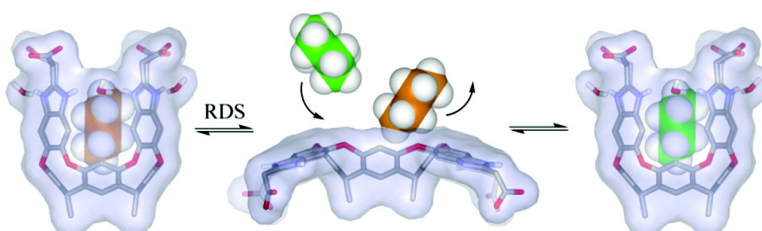
Article

Extraction of Hydrophobic Species into a Water-Soluble Synthetic Receptor

Richard J. Hooley, Hillary J. Van Anda, and Julius Rebek

J. Am. Chem. Soc., **2007**, 129 (44), 13464-13473 • DOI: 10.1021/ja0727058 • Publication Date (Web): 10 October 2007

Downloaded from <http://pubs.acs.org> on February 14, 2009



More About This Article

Additional resources and features associated with this article are available within the HTML version:

- Supporting Information
- Links to the 10 articles that cite this article, as of the time of this article download
- Access to high resolution figures
- Links to articles and content related to this article
- Copyright permission to reproduce figures and/or text from this article

[View the Full Text HTML](#)

Extraction of Hydrophobic Species into a Water-Soluble Synthetic Receptor

Richard J. Hooley, Hillary J. Van Anda, and Julius Rebek, Jr.*

Contribution from The Skaggs Institute for Chemical Biology and the Department of Chemistry, The Scripps Research Institute, MB-26, 10550 North Torrey Pines Road, La Jolla, California 92037

Received April 18, 2007; E-mail: jrebek@scripps.edu

Abstract: A deep, water-soluble cavitand extracts a variety of neutral hydrophobic species into its cavity. Flexible species such as *n*-alkanes tumble rapidly on the NMR time scale inside the cavity, but this motion is slowed for bulkier guests. Long, rigid guests such as *p*-substituted aromatics are either static or only tumble at elevated temperatures *via* flexing motions of the cavitand. Strong selectivity in recognition of long rigid guests is seen. The binding of neutral guests occurs *via* the classical hydrophobic effect; the process is entropically favored, as shown by isothermal titration calorimetry measurements. Binding affinities are generally on the order of 10^4 – 10^5 M⁻¹. The extent of the hydrophobic stabilization is shown by the binding of long trimethylammonium salts, which bind the alkyl chain in the cavity, rather than the NMe₃⁺ group. Dynamic NMR studies show that self-exchange of neutral guests is independent of guest concentration, and most likely occurs *via* rate-determining unfolding of the cavitand. In the absence of guests, the cavitand exists in a dimeric velcrand structure.

1. Introduction

The hydrophobic effect is one of the strongest driving forces for molecular recognition in water,^{1–4} and biological systems have inspired the construction of many synthetic receptors with hydrophobic interiors. Fatty acid binding proteins (FABPs) and nonspecific lipid-transfer proteins are examples of natural receptors that provide sizable hydrophobic cavities to surround their guests, and these guests can assume unpredictable shapes in the host/guest complexes.^{5–7} Hydrocarbons and other hydrophobic groups behave similarly in the cavity of synthetic receptors. They can flex and adapt to the surface of the cavity to fill the available space properly, maximize the attractive contacts, and escape from water. For example, the behavior of *n*-alkanes and haloalkanes when confined in the restricted cavity of calixarenes,⁸ cyclodextrins, and self-assembled capsules^{9–11} reveals kinked and coiled conformations.¹² Rigid aromatic hydrocarbons have been extracted into aqueous solutions of

cationic cyclophane-based receptors^{13,14} and metal–ligand clusters through hydrophobic effects.^{15–18}

In this report we narrow the perspective to hydrophobic effects in the context of the water-soluble cavitand **1**.¹⁹ It features aromatic walls that present polarizable π surfaces to the cavity and provide stabilizing effects to cations^{21,22} and molecules bearing a thin layer of positive charge such as C–H bonds. It also binds charged, water-soluble guests,²⁰ and even anionic species such as surfactants sodium dodecyl sulfate (SDS) and dodecyl phosphocholine (DPC) bind at concentrations below their critical micelle concentration.^{23,24} These lipids position their hydrocarbon tails inside the cavity and coil them into a helical shape so as to optimally fill the space inside and leave the hydrophilic head in the water layer. The binding of a wide variety of neutral, water-insoluble species by **1** in aqueous solution is reported here.²⁵

- (1) Tanford, C. *Science* **1978**, *200*, 1012–1018.
- (2) Tanford, C. H. In *The Hydrophobic Effect: Formation of Micelles and Biological Membranes*; Wiley: New York, 1980.
- (3) Pratt, L. R.; Pohorille, A. *Chem. Rev.* **2002**, *102*, 2671–2692.
- (4) Sutherland, I. O. *Chem. Soc. Rev.* **1986**, *15*, 63–91.
- (5) Zimmerman, A. W.; Veerkamp, J. H. *Cell Mol. Life Sci.* **2002**, *59*, 1096–1116.
- (6) Zanotti, G.; Scapin, G.; Spadon, P.; Veerkamp, J. H.; Sacchettini, J. C. *J. Biol. Chem.* **1992**, *267*, 18541–18550.
- (7) Han, G. W.; Lee, J. Y.; Song, H. K.; Chang, C. S.; Min, K.; Moon, J.; Shin, D. H.; Kopka, M. L.; Sawaya, M. R.; Yuan, H. S.; Kim, T. D.; Choe, J.; Lim, D.; Moon, H. J.; Suh, S. W. *J. Mol. Biol.* **2001**, *308*, 263–278.
- (8) Brouwer, E. B.; Udachin, K. A.; Enright, G. D.; Ripmeester, J. A.; Ooms, K. J.; Halchuk, P. A. *Chem. Commun.* **2001**, 565–566.
- (9) Scarso, A.; Trembleau, L.; Rebek, J. *Angew. Chem., Int. Ed.* **2003**, *42*, 5499–5502.
- (10) Gibb, C. L. D.; Gibb, B. C. *J. Am. Chem. Soc.* **2004**, *126*, 11408–11409.
- (11) Gibb, C. L. D.; Gibb, B. C. *J. Am. Chem. Soc.* **2006**, *128*, 16498–16499.
- (12) Schramm, M. P.; Rebek, J., Jr. *Chem.–Eur. J.* **2006**, *12*, 5924–5933.

- (13) Diederich, F.; Dick, K. *J. Am. Chem. Soc.* **1984**, *106*, 8024–8036.
- (14) Diederich, F.; Griebel, D. *J. Am. Chem. Soc.* **1984**, *106*, 8037–8046.
- (15) Yoshizawa, M.; Tamura, M.; Fujita, M. *Science* **2006**, *312*, 251–254.
- (16) Yoshizawa, M.; Kusakawa, T.; Fujita, M.; Sakamoto, S.; Yamaguchi, K. *J. Am. Chem. Soc.* **2001**, *123*, 10454–10459.
- (17) Fujita, M.; Umamoto, K.; Yoshizawa, M.; Fujita, N.; Kusakawa, T.; Biradha, K. *Chem. Commun.* **2001**, 509–518.
- (18) Yoshizawa, M.; Tamura, M.; Fujita, M. *J. Am. Chem. Soc.* **2004**, *126*, 6846–6847.
- (19) Hof, F.; Trembleau, L.; Ullrich, E. C.; Rebek, J. *Angew. Chem., Int. Ed.* **2003**, *42*, 3150–3153.
- (20) Biros, S. M.; Ullrich, E. C.; Hof, F.; Trembleau, L.; Rebek, J. *J. Am. Chem. Soc.* **2004**, *126*, 2870–2876.
- (21) Petti, M. A.; Shepodd, T. J.; Barrans, R. E.; Dougherty, D. A. *J. Am. Chem. Soc.* **1988**, *110*, 6825–6840.
- (22) Kearney, P. C.; Mizoue, L. S.; Kumpf, R. A.; Forman, J. E.; McCurdy, A.; Dougherty, D. A. *J. Am. Chem. Soc.* **1993**, *115*, 9907–9919.
- (23) Trembleau, L.; Rebek, J., Jr. *Science* **2003**, *301*, 1219–1220.
- (24) Trembleau, L.; Rebek, J., Jr. *Chem. Commun.* **2004**, 58–59.
- (25) A portion of this work has been previously communicated: Hooley, R. J.; Biros, S. M.; Rebek, J. *Chem. Commun.* **2006**, 509–510.

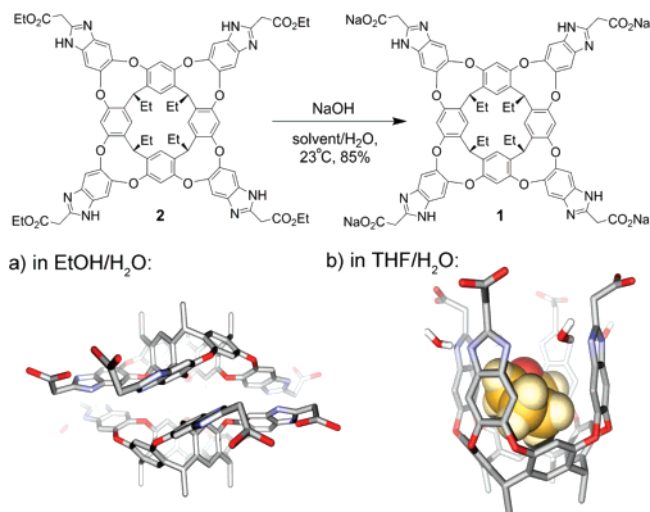


Figure 1. Synthesis of the water-soluble tetracarboxylate cavitand **1** and (a) a representation of the dimeric complex of **1** when synthesized by saponification in EtOH/H₂O and (b) a representation of the complex of **1** with bound THF when synthesized by saponification in THF/H₂O (Maestro v7.0.2; AMBER forcefield;²⁶ some groups omitted for clarity).

2. Cavitand Structure

Cavitand **1** is prepared by saponification of the corresponding tetraethyl ester **2** in THF/H₂O, and is isolated with one molecule of THF occupying the cavity.²⁰ The cavity retains a THF guest so as to remain folded and avoid either a vacuum or the unfavorable interactions between water and the aromatic interior. Removal of THF from the cavity, even under extreme conditions of heat and high vacuum, cannot be achieved.²⁰ The cavitand exists in a kinetically stable (on the NMR time scale) “vase” conformation in solution, held together by four water molecules on the upper rim that provide hydrogen bonds to the benzimidazoles (Figure 1b).²⁷ This is the only form observed in solution, and the limit of concentration is about 20 mM.

In order to access the “empty” structure, saponification of the precursor tetraethyl ester cavitand **2** was performed in EtOH/H₂O instead of THF/H₂O. On isolation, the ¹H NMR spectrum of the cavitand was observed to be significantly different than that from saponification in THF/H₂O (Figure 2). Two sets of peaks are present; the minor species corresponds to a folded vase conformation, most likely binding one molecule of EtOH. The major species shows the characteristic methine proton H_d as a doublet of doublets at 3.97 ppm, indicative of a “kite” conformation of two-fold symmetry.²⁸ The ¹H NMR spectra do not distinguish between a dimer of (average) *D*_{2d} symmetry or a monomer of (average) *C*_{4v} symmetry, but electrospray mass spectrometric analysis showed the presence of a dimeric complex of mass 2577.77 (corresponding to the octa-acid dimer after ionization in a positive matrix). The solution structure is a dimeric velcra complex of *D*_{2d} symmetry (Figure 1a).²⁹ The monomeric kite form exposes a larger hydrophobic surface area to the aqueous environment, and dimerization effectively reduces

its unfavorable interactions with solvent. Diffusion ordered spectroscopy (DOSY) experiments were also performed.^{30–32} The monomeric THF-containing cavitand **1** gave a diffusion constant of 2.41×10^{-10} m²/s, whereas the larger dimeric velcra complex **1•1** diffused more slowly ($D = 2.17 \times 10^{-10}$ m²/s), as might be expected from the larger mass and greater negative charge. The forces that hold the dimer together are weak (indeed, one equivalent of THF breaks the complex apart). The guest binding properties of the dimeric complex were identical to that of the THF-containing monomer, and (unless stated otherwise) all binding studies described here were performed on the monomeric THF-containing cavitand.

3. Extraction and Binding of Normal Alkanes

The binding of SDS mentioned above suggested that other flexible hydrocarbons could be good guests, and this was the case.³³ A 2 mM solution of cavitand **1** was exposed to an excess of a variety of *n*-alkanes (methane–dodecane **3–14**). Extraction of the smaller guests proved extremely facile—the gases were bubbled into the solution of **1** for 2 min, and the liquids were merely added as one drop. The smallest alkanes methane **3** and ethane **4** were not bound, presumably because they are too small to effectively occupy the cavity. The larger alkanes form 1:1 complexes with the host. The bound guests are revealed by their characteristic upfield ¹H NMR resonances imparted by the anisotropic magnetic shielding properties of the eight aromatic rings.³⁴ Guest binding is quite strong—apparent binding constants $> 10^4$ M⁻¹ were calculated from the NMR spectra, and in the case of *n*-butane through *n*-octane, no free guest was observed; the cavitand extracted only as much as it could accommodate. Figure 3 shows the upfield portion of the ¹H NMR spectra of the complexes of *n*-alkanes bound in **1**. The spectrum of SDS is also provided as a reference. It is clear that the *n*-alkanes do not bind in the same manner as SDS. The cavitand provides a gradient of magnetic anisotropy that shifts the residues bound deepest in the cavity the furthest upfield;³⁴ the spectrum of SDS illustrates this. The terminal methyl group is bound as deep as its shape allows in the tapered end of the cavity ($\Delta\delta \approx -5$ ppm), and the penultimate methylene residue is less shifted. Each subsequent methylene is monotonically less upfield shifted, and a total of eight residues are affected; residues 9–12 are unshifted. A maximum of 8 carbons can be buried in a helical conformation, and no more than 5 carbons in an extended one. By contrast, the spectra for the *n*-alkanes look quite different. Propane **5**, *n*-butane **6**, and *n*-pentane **7** are bound, but their upfield signals are broad and undefined, presumably due to a relatively fast in/out exchange rate.¹¹ *n*-Hexane through *n*-dodecane (**8–14**) show individual signals that are broadened and clustered at smaller $\Delta\delta$ than would be expected for a static helical conformation. The chemical shifts indicate that the alkanes are not only coiled in a helical conformation but are *tumbling rapidly* on the NMR time scale. The spectra of *n*-butane and *n*-pentane are too broad to interpret, but for **8–14** each of the methyls and methylenes of the alkanes show an averaged chemical shift

(26) Mohamadi, F.; Richards, N. G. J.; Guida, W. C.; Liskamp, R.; Lipton, M.; Caufield, C.; Chang, G.; Hendrickson, T.; Still, W. C. *J. Comput. Chem.* **1990**, *11*, 440–467.

(27) Far, A. R.; Shivanyuk, A.; Rebek, J., Jr. *J. Am. Chem. Soc.* **2002**, *124*, 2854–2855.

(28) Moran, J. R.; Ericson, J. L.; Dalcanale, E.; Bryant, J. A.; Knobler, C. B.; Cram, D. J. *J. Am. Chem. Soc.* **1991**, *113*, 5707–5714.

(29) Haino, T.; Rudkevich, D. M.; Shivanyuk, A.; Rissanen, K.; Rebek, J. *Chem.-Eur. J.* **2000**, *6*, 3797–3805.

(30) Price, W. S. *Concepts Magn. Reson.* **1997**, *9*, 299–336.

(31) Cohen, Y.; Avram, L.; Frish, L. *Angew. Chem., Int. Ed.* **2005**, *44*, 520–524.

(32) Avram, L.; Cohen, Y. *J. Am. Chem. Soc.* **2005**, *127*, 5714–5719.

(33) Hoolley, R. J.; Rebek, J., Jr. *Org. Lett.* **2007**, *9*, 1179–1182.

(34) Menozzi, E.; Onagi, H.; Rheingold, A. L.; Rebek, J. *Eur. J. Org. Chem.* **2005**, 3633–3636.

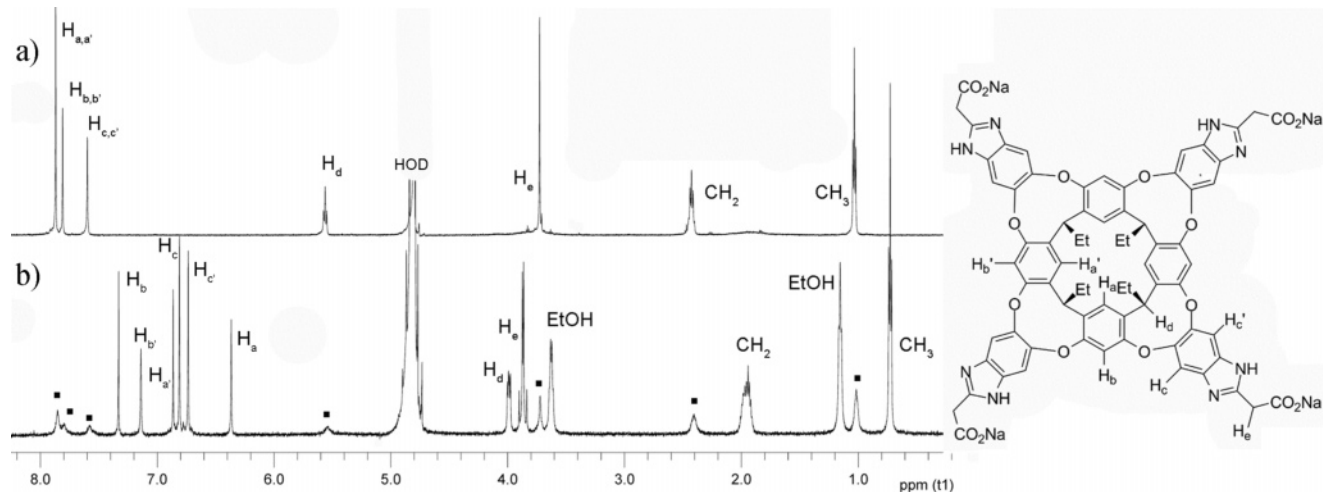


Figure 2. ^1H NMR spectra (2 mM, D_2O) of the two forms of water-soluble tetracarboxylate cavitand; (a) $\mathbf{1}\cdot\text{THF}$ (C_{4v} monomer) and (b) $\mathbf{1}\cdot\mathbf{1}$ (D_{2d} dimer). ■ = minor complex $\mathbf{1}\cdot\text{EtOH}$.

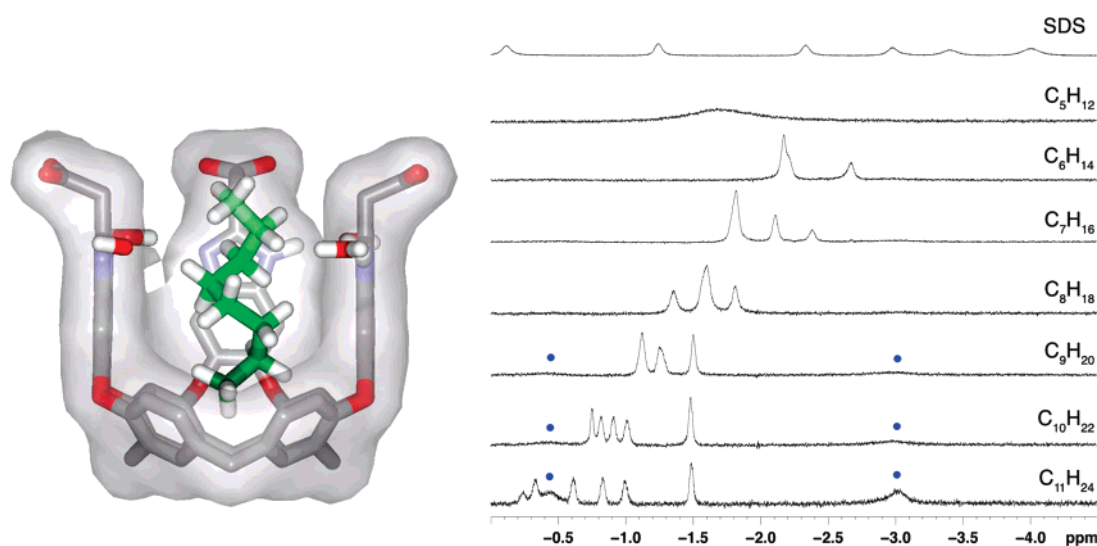


Figure 3. Representation of the complex of $\mathbf{1}$ with coiled *n*-octane (Maestro v7.0.2; AMBER forcefield;²⁶ some groups omitted for clarity). Upfield regions of ^1H NMR spectra of sodium dodecyl sulfate (SDS) and *n*-alkanes (C_5H_{12} to $\text{C}_{11}\text{H}_{24}$) in a 2 mM solution of $\mathbf{1}$ in D_2O . (●): encapsulated THF.

of two different magnetic environments. Figure 4 shows the expected chemical shifts of each residue bound in cavitand $\mathbf{1}$ (derived from the observed chemical shifts of SDS). The NMR signals of the exposed, terminal groups of *n*-nonane through *n*-dodecane would be unshifted by binding, and the observed NMR spectra can be calculated by averaging the chemical shift of the two relevant residues (e.g., for *n*-octane, $\text{C}_1 + \text{C}_8$ and $\text{C}_2 + \text{C}_7$ show the same $\Delta\delta$, etc.; see Supporting Information for analysis).

n-Nonane and longer alkanes are increasingly poor guests—signals for competing bound THF are observed, indicating incomplete extraction of the alkane. Only after several days of sonication can any bound dodecane be seen. Unlike SDS, with its polar sulfate group that is fixed in the water solvent, the *n*-alkanes are free to move in the cavity. As the alkanes get larger than C_8 , they can no longer fit completely inside the cavity, and the benefits of burying the hydrophobic surfaces are diminished. Accordingly, the displacement of THF from the cavity becomes less favorable, and the amount of alkane extracted decreases. For the larger alkanes, broad signals for free guest can be seen due to the formation of micellar

aggregates; the reduced binding affinity is most likely not due to a decrease in guest solubility.

Branched alkanes are guests also but show slower tumbling and broad, undefined NMR signals at 300 K. The temperature-dependent spectra of 2,2-dimethylpentane $\mathbf{15}$ and 2,2-dimethylhexane $\mathbf{16}$ are shown in Figure 5. The small 2,2-dimethylpentane is unaffected by temperature and shows relatively sharp peaks, but larger $\mathbf{16}$ shows broad peaks at 300 K, and these only sharpen at higher temperature. Monosubstituted alkanes show similar behavior. Evidently 2-methylpentane and 2,2-dimethylpentane are small enough to rotate freely and display sharp, averaged peaks in their spectra. The longer alkanes, 2-methylhexane and 2,2-dimethylhexane, do not have enough space to allow the large isopropyl and *tert*-butyl groups, respectively, to tumble in the cavity. Isooctane (2,2,4-trimethylpentane) also shows sharp averaged signals in the ^1H NMR spectrum due to rapid tumbling.

4. Cyclic Hydrocarbons

For linear alkanes, helical coiling is necessary to appropriately fill the available space, but cyclic hydrocarbons already feature

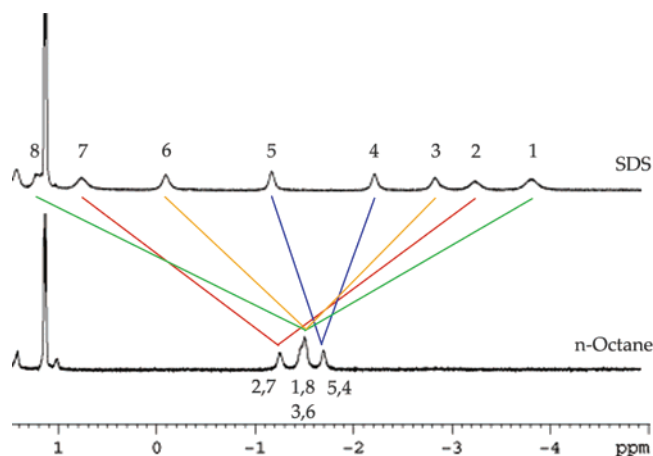


Figure 4. Averaging of the position of tumbling helical alkane residues in **1** correlated with $\Delta\delta$.

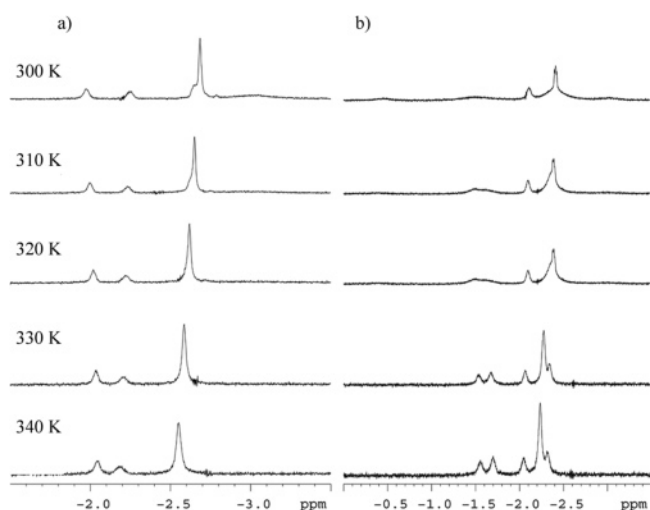


Figure 5. Temperature dependence of the ^1H NMR spectra of (a) 2,2-dimethylpentane **15** and (b) 2,2-dimethylhexane **16** in a 2 mM solution of **1** (D_2O).

shapes that can do so.³⁵ For cycloalkanes C_5H_{10} to $\text{C}_{10}\text{H}_{20}$, stoichiometric extraction was observed under mild conditions. These cycloalkanes show some solubility in water, and free guest can be observed, although the binding constants for each of the tested guests were above the 10^4 M^{-1} limit accessible from ^1H NMR integration. The complex between cyclopentane and **1** shows a broad singlet in the upfield region of the ^1H NMR spectrum, and the cycloalkanes C_6H_{12} to $\text{C}_{10}\text{H}_{20}$ show one sharp singlet, indicating that they are tumbling rapidly on the NMR time scale (see Supporting Information). Cyclohexane is the best guest for the cavity, as shown by competition experiments (Table 2). It was assumed that the binding constants were significantly larger than that of THF (as all THF is expunged from the cavity upon alkane binding), and so the binding of THF was not included in the calculation of relative binding affinities. The preference for C_6 over C_5 and C_7 is not large, whereas cyclooctane and cyclodecane show much lower binding affinities. The acyclic alkanes show lower binding affinities than cyclohexane, and they decrease as the guest size increases. The volume of the cavity can be estimated *via* molecular modeling to be 180 \AA^3 by fixing an artificial lid at the level of the

Table 1. Averaging of the Position of Tumbling Helical Alkane Residues in **1** Correlated with $\Delta\delta$

SDS	<i>n</i> -heptane 9		<i>n</i> -octane 10		<i>n</i> -decane 12		
	Δ_{observed}	$\Delta_{\text{predicted}}$	Δ_{observed}	$\Delta_{\text{predicted}}$	Δ_{observed}	$\Delta_{\text{predicted}}$	
C_1	-3.95						
C_2	-3.35						
C_3	-2.95						
C_4	-2.30	$\text{C}_{1/7}$ -1.83	-1.80	$\text{C}_{1/8}$ -1.63	-1.59	$\text{C}_{1/10}$ -1.58	-1.48
C_5	-1.30	$\text{C}_{2/6}$ -1.78	-1.80	$\text{C}_{2/7}$ -1.33	-1.35	$\text{C}_{2/9}$ -1.08	-1.00
C_6	-0.20	$\text{C}_{3/5}$ -2.13	-2.10	$\text{C}_{3/6}$ -1.58	-1.59	$\text{C}_{3/8}$ -0.93	-0.91
C_7	0.70	C_4 -2.40	-2.37	$\text{C}_{4/5}$ -1.80	-1.83	$\text{C}_{4/7}$ -0.80	-0.80
C_8	1.10					$\text{C}_{5/6}$ -0.75	-0.75
C_9	1.20						
C_{10}	1.20						

Table 2. Competitive Binding of Cyclohexane **17** and Other Cyclic Alkanes in **1**

guest	K_{rel} ($\text{c-C}_6\text{H}_{12}$)	K_{rel} ($\text{n-C}_6\text{H}_{14}$)	guest volume/ \AA^3	packing coefficient
cyclopentane	0.74		86	0.48
cyclohexane	1		102	0.57
cycloheptane	0.55		117	0.65
cyclooctane	0.28		135	0.75
cyclodecane	0.15		168	0.93
<i>n</i> -hexane	0.33	1	113	0.63
<i>n</i> -heptane	0.18	0.39	126	0.70
<i>n</i> -octane	0.08	0.18	137	0.76
<i>iso</i> -octane	0.35	1.03	135	0.75

carboxylate methylene groups on the rim, and this volume is used for the calculations of Table 2. Strongest binding in systems such as these is usually observed when the guest has the shape complementarity for the host and an appropriate size; a packing coefficient of 0.55 is optimum for filling space in the liquid phase.³⁶ The computed van der Waals volume of cyclohexane is 102 \AA^3 , leading to a very favorable packing coefficient of 0.57. Cyclopentane (86 \AA^3) gives a packing coefficient of 0.48; the guest is too small to adequately fill the cavity.³⁷ The larger guests might be conformationally constrained inside the cavity, but it is likely that the cavitation walls flex a certain amount to allow free motion of the guest.³⁸ The weak hydrogen-bonded forces holding the walls together would allow such motions and increase the volume of the host accordingly.

In contrast, rigid guests such as aromatic rings cannot alter their conformations, and so their binding in the cavity is weakened. Accordingly, small aromatic guests show only slight affinity for the cavitation. The ^1H NMR signals for free benzene and furan in water are slightly broadened and shifted upfield in the presence of cavitation **1**, but the in/out exchange rates are too fast to observe separate signals for the bound complex. Less water-soluble guests such as toluene, *p*-xylene, azulene, and naphthalene show no sharp peaks for either free or bound guest. The ^1H NMR spectra of their complexes with 1 mM **1** in D_2O exhibit shifts and broadening in the peaks for cavitation (Figure 6), as well as signals for free THF, indicating its expulsion from the cavity by the added guests. Evidently a small (\sim mM) concentration of guest is in exchange at an intermediate rate between the cavity and bulk solvent.

(36) Mecozzi, S.; Rebek, J. *Chem.-Eur. J.* **1998**, *4*, 1016–1022.

(37) Gottschalk, T.; Jaun, B.; Diederich, F. *Angew. Chem., Int. Ed.* **2007**, *46*, 260–264.

(38) Scarso, A.; Onagi, H.; Rebek, J. *J. Am. Chem. Soc.* **2004**, *126*, 12728–12729.

(35) Hooley, R. J.; Van Anda, H. J.; Rebek, J. *J. Am. Chem. Soc.* **2006**, *128*, 3894–3895.

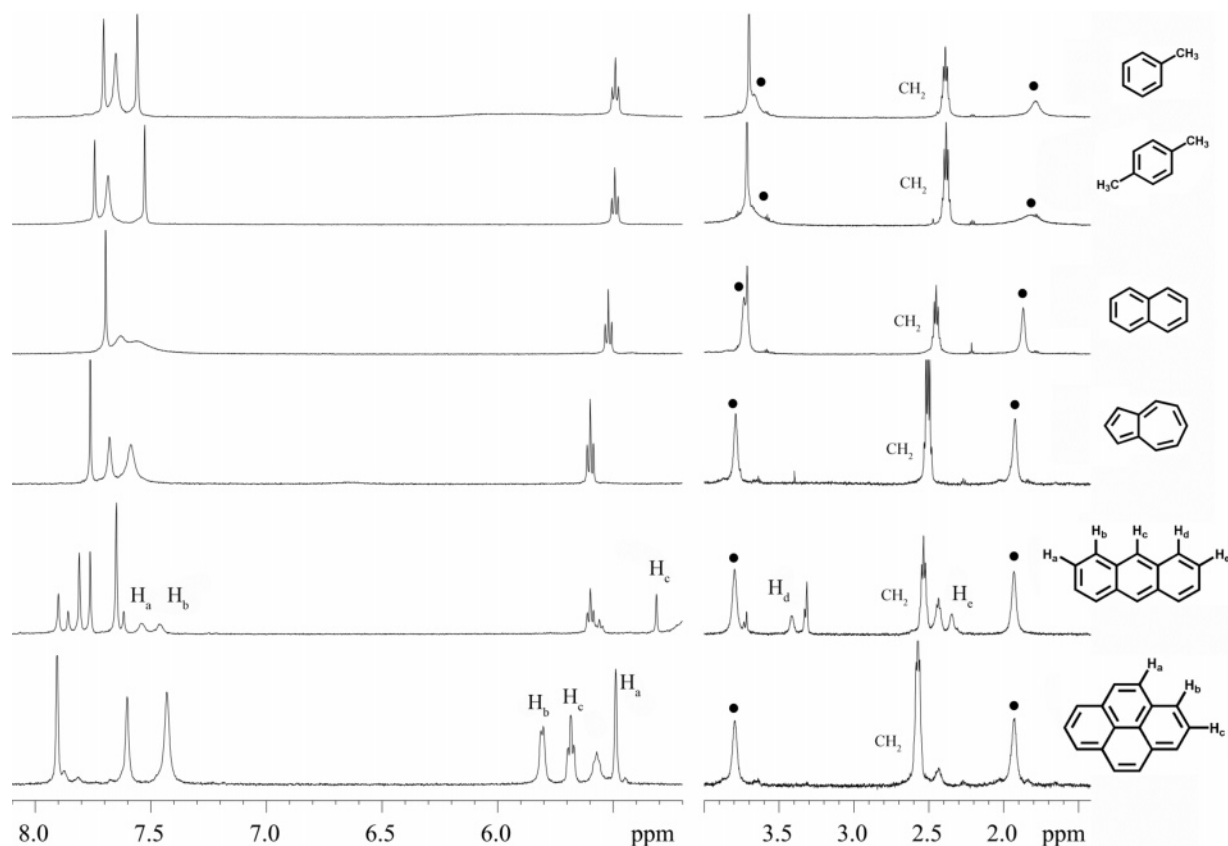


Figure 6. Downfield region of the ^1H NMR spectra (2 mM, D_2O) of the complexes between **1** and various rigid aromatic guests. ● = free THF, expunged from cavitand **1**.

Low-temperature NMR experiments that would be desirable in order to freeze out this motion are precluded by the high melting point of D_2O . Spectra acquired at 280 K were not appreciably different from those at ambient temperature. When larger guests were introduced to the cavity, the picture became clearer. At 300 K, the complex **1**•anthracene shows quite broad, undefined peaks, but cooling to 280 K reveals distinct assignable peaks for bound guest. This increase in kinetic stability of the complex can be ascribed to either (or both) a decrease in water solubility or an increase in the number of favorable $\text{CH}-\pi$ interactions of the larger guest with the cavity. At 280 K, anthracene does not tumble, and five distinct guest signals are shown, ranging in δ from 7.5 ppm (unshifted, residing above the cavitand rim) to 3.8 ppm (highly shifted, residing near the resorcinarene base). The complex between **1** and the shorter but wider pyrene is kinetically stable at 300 K, although in this case the guest is observed to tumble and only three averaged signals at δ 5.8, 5.7, and 5.5 ppm are seen. Obviously the host breathes to accommodate this tumbling.³⁸

Long, rigid substrates with appended methyl or *tert*-butyl groups are also good guests, due to favorable $\text{CH}-\pi$ interactions with the resorcinarene base. The ^1H NMR spectra of the complexes of 4,4'-dimethylbiphenyl **18** and 1,4-di-*tert*-butylbenzene **19** are shown in Figure 7. As expected, extraction of these highly insoluble solids into aqueous solution requires harsher conditions than for the liquid hydrocarbons—sonication for a period of at least 12 h was required for complete displacement of resident THF. Even after 24 h, complete extraction of **19** is not achieved. In both cases, the guest does

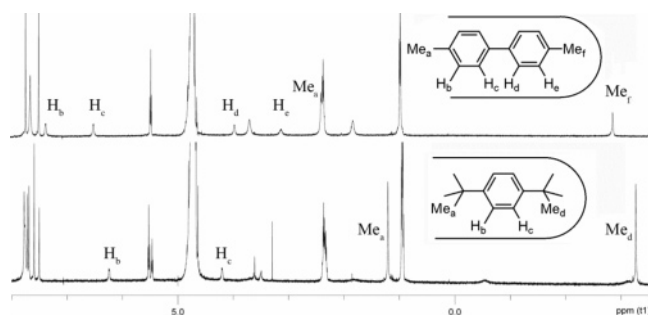


Figure 7. ^1H NMR spectra (2 mM, D_2O) of the complexes between **1** and 4,4'-dimethylbiphenyl **18** and 1,4-di-*tert*-butylbenzene **19**.

not exhibit rapid tumbling due to its rigidity and length; all of the ^1H signals can be distinguished in the NMR spectra.

5. Motion Inside the Cavity

The binding characteristics of the cavitand are nonspecific; there are no directed interactions between host and guest, merely London dispersion forces and $\text{CH}-\pi$ interactions. Consequently, the number of favorable guest conformations is large, and flexible guests can interconvert between these conformations inside the cavity without loss of attractive contacts to the cavitand. Figure 8a shows a “snaking” motion *via* a chairlike, U-shaped intermediate where one end of the alkane moves past the other, to the inverted helix shown. “Rotation” is illustrated in Figure 8b and describes the motion of the hydrocarbon without bending that is applicable only to short hydrocarbons. When branching is present on the alkyl chain, the snaking motion of an isopropyl or *tert*-butyl group past the coiled chain

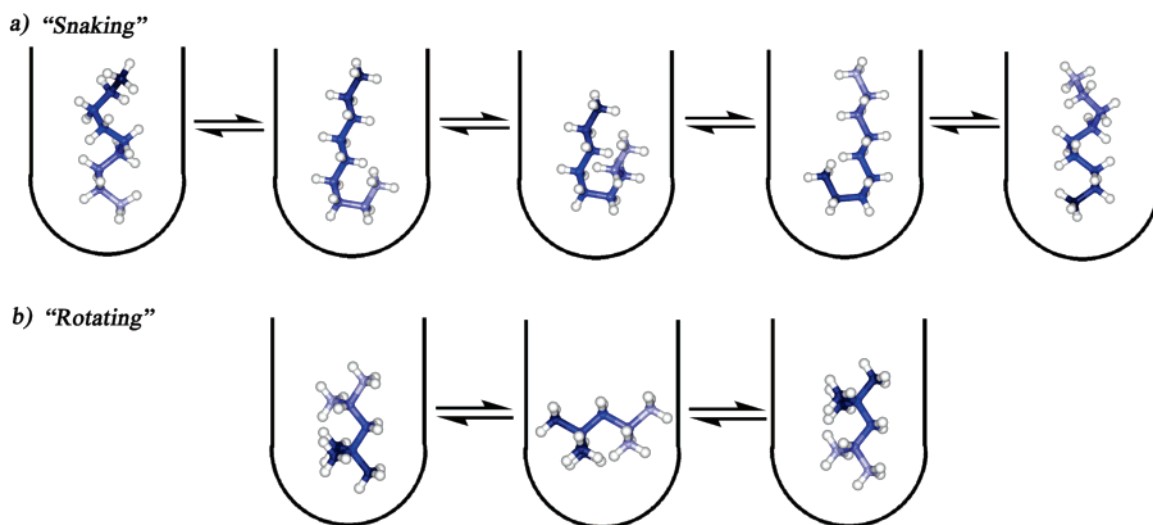


Figure 8. Proposed modes of alkane tumbling.

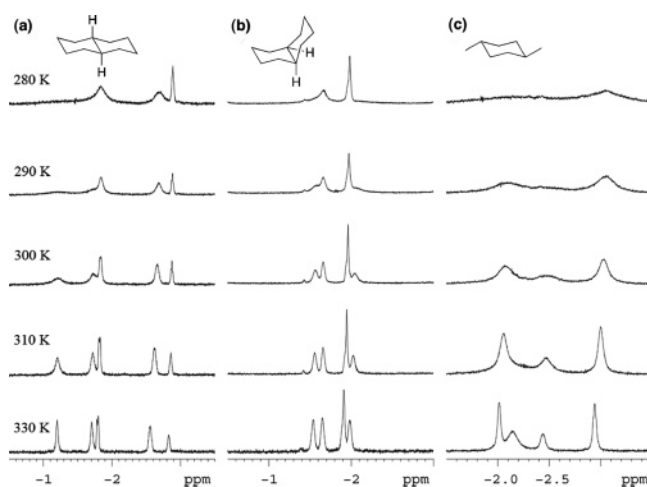


Figure 9. Temperature dependence of the ^1H NMR spectra of (a) *trans*-decalin **23**, (b) *cis*-decalin **22**, and (c) *trans*-1,4-dimethylcyclohexane **21** in a 1.5 mM solution of **1** in D_2O .

is inhibited by the space constraints of the cavity. Accordingly, only substituted alkanes with longest linear chain length of five carbons (isooctane, 2-methylpentane) move rapidly on the NMR time scale at ambient temperature, and they probably do so *via* rotation of the molecule as a whole.

The mobility of more rigid guests, *cis*- and *trans*-1,4-dimethylcyclohexane (**20**, **21**) and *cis*- and *trans*-decalin (**22**, **23**), was examined. All were extracted and formed stoichiometric complexes with **1**. *cis*-1,4-Dimethylcyclohexane is small enough to rotate rapidly in the cavity, but encapsulation of *trans*-1,4-dimethylcyclohexane and both decalin isomers leads to complexes that exhibit broad peaks for bound guest, similar in nature to those observed for the substituted acyclic alkanes. In these cases, however, the guest cannot “snake” and the cavitand must flex instead. The effect of temperature on the ^1H NMR spectra of these complexes is shown in Figure 9. Upon heating, the signals for encapsulated guest sharpen considerably, indicating that at ambient temperature, rotations occur on an intermediate NMR chemical shift time scale. *cis*-Decalin is shorter and more flexible than *trans*-decalin, so a lower temperature is required for rapid rotation.

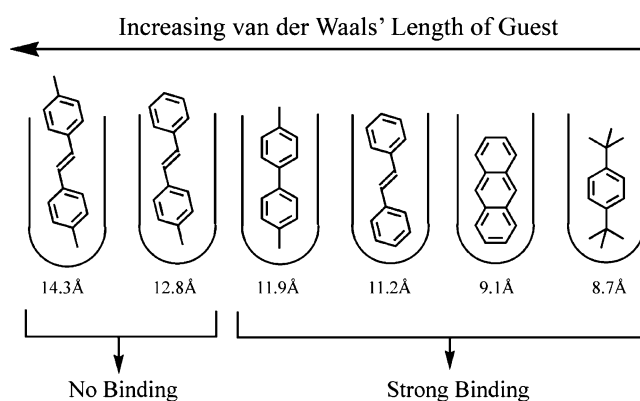


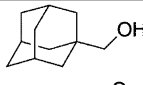
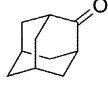
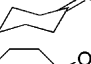
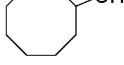
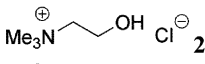
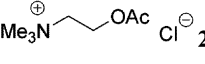
Figure 10. Representation of the binding characteristics of the “molecular ruler”.

The aryl guests anthracene, 4,4'-dimethylbiphenyl **18**, and 1,4-di-*tert*-butylbenzene **19** did not show rapid rotation inside **1**. The cavitand acts as a molecular ruler—there is a distinct cutoff for the length of a rigid guest that can be extracted into the cavity (see Figure 10). 4,4'-Dimethylbiphenyl is the longest guest bound, with a van der Waals length of 11.9 Å. Stilbene (11.2 Å) is bound (although it displays the same type of ^1H NMR spectrum as anthracene, *vide supra*), but methylstilbene (12.7 Å) and 4,4'-dimethylstilbene (14.3 Å) are not extracted into the cavitand even after several days of sonication. If the rigid guest protrudes beyond the cavitand rim, unfavorable interactions between solvent water and the guest's hydrophobic surface disrupt the energetic balances of the binding event. Flexible guests such as *n*-alkanes can vary their shape in order to expose the minimum amount of surface area to the solvent—hence, the slow dropoff in binding affinity as these guests are lengthened. While *n*-octane reaches the cavity's rim, alkanes as long as *n*-dodecane show binding. In contrast, the addition of only 0.9 Å in length to 4,4'-dimethylbiphenyl completely abrogates binding, a remarkable behavior for an open-ended container molecule.

6. Thermodynamics and Kinetics of Guest Exchange

Investigation of the exchange properties of these hydrophobic guests is complicated somewhat by their strong binding and low water solubility. Fortunately, certain guests display suffi-

Table 3. Thermodynamic Binding Parameters (ITC) of Guests in Cavitand **1**

Guest	K/M^{-1}	$\Delta H,$ kcal mol^{-1}	$\Delta S,$ $\text{cal mol}^{-1} \text{K}^{-1}$
 24	2.9×10^5	-2.0	18.4
 25	1.3×10^5	-3.4	11.9
 26	1.6×10^5	-4.0	10.0
 27	2.6×10^5	-2.4	16.8
 28 ²⁰	2.6×10^4	-9.0	-10
 29 ²⁰	1.2×10^4	-4.5	3.7

cient solubility in water to allow thermodynamic analysis by isothermal titration calorimetry (ITC) and kinetic analysis by 2D EXSY NMR. Table 3 shows the thermodynamic binding properties of five suitable neutral guests, each containing a large cyclic hydrocarbon anchor and a slightly polar group for added water solubility. In each case, the adamantyl/cycloalkyl group binds inside the cavitand, with the hydroxyl/carbonyl group oriented to the aqueous solution (see Supporting Information for NMR data). Guests **24–27** have solubilities on the order of 10^1 – 10^2 mM in water, allowing titration of a stock solution into the ITC cell. Previously published parameters for charged choline and acetylcholine are included in the table as reference points.

The neutral hydrophobic guests bind *via* a classical hydrophobic effect in cavitand **1**. Binding is strongly entropy-driven, with a small favorable enthalpic term. The entropic benefit is due to release of ordered water from the surface of the hydrophobic neutral species on binding that causes a net increase in disorder. The ΔC_p value for the self-exchange of cyclooctanol in **1** was strongly negative ($\Delta C_p = -250 \text{ cal mol}^{-1} \text{K}^{-1}$) as expected for classical hydrophobic binding. This cavitand evidently does not behave in the non-classical manner observed by Diederich in synthetic receptors^{39–42} (which can also be seen in membranes⁴³). In the latter, charged water-soluble receptors showed strong hydrophobic binding due mainly to an *enthalpic* bonus gained on hydrocarbon binding. The cavitand walls are moderately good matches for the hydrocarbon guest in terms of London dispersion forces consistent with the weaker binding of hydrocarbons in neutral cavitands of this type in organic solutions. The overall binding energy is large (average $K \approx 1 \times 10^5 \text{ M}^{-1}$ (Table 3), $\Delta G \approx 7 \text{ kcal mol}^{-1}$, consistent with ¹H NMR measurements), almost an order of magnitude stronger than the binding of choline ($K = 2.6 \times 10^4 \text{ M}^{-1}$). The charged

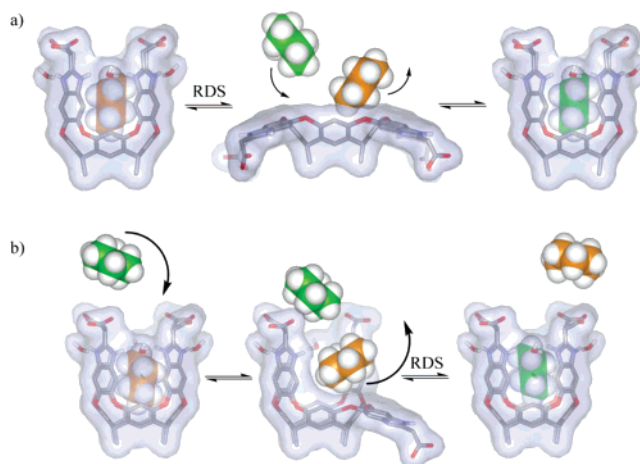
(39) Smithrud, D. B.; Sanford, E. M.; Chao, I.; Ferguson, S. B.; Carcanague, D. R.; Evansck, J. D.; Houk, K. N.; Diederich, F. *Pure Appl. Chem.* **1990**, *62*, 2227–2236.

(40) Ferguson, S. B.; Seward, E. M.; Diederich, F.; Sanford, E. M.; Chou, A.; Inocenciosweda, P.; Knobler, C. B. *J. Org. Chem.* **1988**, *53*, 5593–5595.

(41) Ferguson, S. B.; Sanford, E. M.; Seward, E. M.; Diederich, F. *J. Am. Chem. Soc.* **1991**, *113*, 5410–5419.

(42) Diederich, F.; Smithrud, D. B.; Sanford, E. M.; Wyman, T. B.; Ferguson, S. B.; Carcanague, D. R.; Chao, I.; Houk, K. N. *Acta Chem. Scand.* **1992**, *46*, 205–215.

(43) Seelig, J.; Ganz, P. *Biochemistry* **1991**, *30*, 9354–9359.

**Figure 11.** Illustrations of the two possible exchange mechanisms: (a) “S_N1-like” and (b) “S_N2-like”.

tetramethylammonium groups allow strong binding of choline by *enthalpically* favorable cation– π interactions; they compensate for either an unfavorable (in the case of choline) or weakly favorable (in the case of acetylcholine) entropic term. The binding of neutral species, however, is more strongly driven by entropic effects. The enthalpic term is much smaller, due to the absence of strong cation– π interactions (again, consistent with the preferential binding of choline vs hydrocarbons in organic solvents).²⁷

The magnitude of this hydrophobic effect is illustrated by the binding of long alkyltrimethylammonium salts. Choline and acetylcholine bind with the trimethylammonium group at the base of the cavity, as do short alkyltrimethylammoniums (EtNMe₃⁺, ⁿBuNMe₃⁺, ⁿHexNMe₃⁺).³⁴ When decyl or dodecyltrimethylammonium bromide are added to a 1 mM solution of **1** in D₂O, binding of the alkyl chain in the expected helical conformation, and *not the trimethylammonium* is observed. This leaves the trimethylammonium group outside the cavity, where it can still interact with the aqueous solvent and the carboxylates at the cavitand rim. The K_a is again $>10^4 \text{ M}^{-1}$, even though each *gauche* interaction that propagates the helix conformation destabilizes the system by 0.5–0.6 kcal/mol.⁴⁴ The increased length of the alkyl chain evidently enhances the entropic binding term and overcomes the unchanged enthalpic interaction of the NMe₃⁺ group with solvent water.

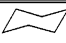

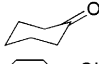
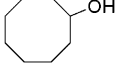
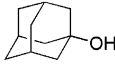

The mechanism of exchange was probed by studying the rate of self-exchange of guests between **1** and bulk solvent. Two general mechanisms have been suggested for exchange processes in self-folding receptors of this type and are illustrated in Figure 11. One possibility is that exchange involves a slow, complete unfolding of cavitand followed by rapid guest exchange occurring from the kite form, in an “S_N1-like” manner. This is the mechanism generally accepted for guest exchange in an organic-soluble octamide cavitand.^{45,46} (A dissociative exchange process that occurs *via* loss of guest from *fully folded* receptor is most unlikely; this creates a vacuum, and the energetic price of this process is expected to be prohibitive.) Analogy can also be drawn with exchange mechanisms for fully enclosed capsules.

(44) Eliel, E. L.; Wilen, S. H. In *Stereochemistry of Organic Compounds*; Wiley: New York, 1994; p 600.

(45) Rudkevich, D. M.; Hilmersson, G.; Rebek, J. *J. Am. Chem. Soc.* **1997**, *119*, 9911–9912.

(46) Rudkevich, D. M.; Hilmersson, G.; Rebek, J. *J. Am. Chem. Soc.* **1998**, *120*, 12216–12225.

Table 4. Exchange Rates of Various Guests (3 mM) between **1** (2 mM) and Bulk Solvent (D₂O)

Guest	k (s ⁻¹)	ΔG [‡] _{in} , kcal mol ⁻¹
 17	14.6	16.0
 30	11.7	16.1
 26	9.8	16.2
 27	3.2	16.9
 32	1.8	17.2
 31	1.7	17.2

It has been shown that, for small molecules such as benzene in a cylindrical capsule,⁴⁷ small cations in a tetrahedral cluster,⁴⁸ and bicyclic hydrocarbons in a spherical capsule,⁴⁹ self-exchange occurs by either opening of one or more “flaps” of the capsule or distortion of a cluster wall to allow an opening. The parallel mechanism in this case can be described as an “S_N2-like” process: opening of one or two walls followed by concerted replacement of bound guest by free. The process is illustrated in Figure 11b. It is not certain (or easily determinable) whether one wall or more needs to open for exchange to occur, but Diederich has shown that exchange can occur *via* opening of two opposite walls in a related cavitand.³⁷

Distinguishing between these two processes involves guest concentration and the exchange rate; the dissociative process would show no dependence on incoming guest, and the concerted process should show first-order dependence on incoming guest concentration. Two-dimensional EXSY experiments^{50,51} were performed on 2 mM solutions of **1** with 3 mM cyclohexane **17**, cyclohexanone **26**, cyclooctanol **27**, norbornadiene **30**, cyclooctadiene **31**, and 1-adamantanol **32** as guests (see Supporting Information for NOESY spectra). The rates and barriers to exchange are shown in Table 4. The observed activation energies for exchange are consistent with previously obtained values for cavitands that self-assemble *via* hydrogen bonding⁴⁶ and vary between 16 and 17.2 kcal mol⁻¹.

Table 4 shows that the rate of self-exchange depends strongly upon the nature of guest, and is not determined solely by the energy required to unfold the cavitand. Previous publications have shown that the barrier to unfolding of a deep cavitand (with no hydrogen-bond stabilization) is of the order of 11 kcal mol⁻¹,⁵³ whereas the barrier to unfolding of a similar cavitand with eight amide groups providing intramolecular hydrogen bonds is 17 kcal mol⁻¹.⁴⁶ While the hydrogen-bonding network

providing stabilization to the vase conformation of **1** is derived from a different source than that of the octamide cavitand, the number of hydrogen bonds is the same, and so one might expect the barrier to unfolding of the cavitand to be of approximately the same magnitude.

Most of the guests in Tables 3 and 4 were not applicable for the determination of concentration dependence due to low water solubility or unsuitable ¹H NMR spectra, but **26**, **27**, and **32** proved cooperative. No change in the rate of self-exchange of cyclohexanone **26** is observed over a 20 mM range in concentration (Figure 12). This indicates that incoming guest is not present in the rate determining step of the exchange mechanism, and the “S_N1-like” dissociative mechanism shown in Figure 11a is dominant.

The self-exchange data for cyclooctanol and adamantanol corroborate this result; while the rate of self-exchange of these species is slower than that of **26**, the rate is again independent of guest concentration, suggesting that cavitand unfolding is the rate-limiting step. This mechanism is also consistent with the variable exchange rate for different guests. The barrier for cavitand unfolding consists *not only* of the breaking of H-bonds but also the loss of enthalpic interactions between host and guest, combined with partial solvation of the guest, all of which vary depending on the hydrophobic surface presented by the guest.

7. Conclusions

A self-folding, water-soluble synthetic receptor has been shown to extract a variety of insoluble guests including normal and substituted alkanes, cyclic and polycyclic, saturated and aromatic hydrocarbons into aqueous solution. Flexible species such as saturated acyclic and cyclic hydrocarbons tumble rapidly on the NMR time scale. Binding constants are in most cases >10⁴ M⁻¹. Guests for which tumbling is restricted show lower binding affinities, and small aromatic species that cannot adequately occupy the space inside the cavity show rapid exchange on the NMR time scale. Long rigid aromatic species form host:guest complexes if their length does not exceed that of the cavitand; once that length is exceeded, binding affinity drops precipitously, leading to exquisite selectivity for certain rigid substrates. Self-exchange, monitored by 2D EXSY experiments, is most likely a dissociative process involving unfolding of the complex as the rate-determining step. Hydrophobic stabilization can be even stronger than cation-π interactions, as shown by the preference of binding a long alkyl chain over a trimethylammonium cation for long-chain alkyltrimethylammonium guests. Applications of these findings to the acceleration of reactions and transport processes are currently underway in our laboratory.

8. Experimental Section

8.1. General Considerations. ¹H, 2D NOESY, and DOSY NMR spectra were recorded on an Avance Bruker DRX-600 spectrometer with a 5-mm QNP probe. Proton (¹H) chemical shifts are reported in parts per million (δ) with respect to tetramethylsilane (TMS, δ = 0), and referenced internally with respect to the protio solvent impurity. Deuterated NMR solvents were obtained from Cambridge Isotope Laboratories, Inc., Andover, MA, and used without further purification. ESI-HRMS data were recorded on an Agilent Electrospray TOF Mass Spectrometer. All added guests were obtained from Aldrich Chemical

(47) Craig, S. L.; Lin, S.; Chen, J.; Rebek, J. *J. Am. Chem. Soc.* **2002**, *124*, 8780–8781.

(48) Davis, A. V.; Fiedler, D.; Seeber, G.; Zahl, A.; van Eldik, R.; Raymond, K. N. *J. Am. Chem. Soc.* **2006**, *128*, 1324–1333.

(49) Santamaria, J.; Martin, T.; Hilmersson, G.; Craig, S. L.; Rebek, J., Jr. *Proc. Natl. Acad. Sci. U.S.A.* **1999**, *96*, 8344–8347.

(50) Perrin, C. L.; Dwyer, T. J. *Chem. Rev.* **1990**, *90*, 935–967.

(51) Zolnai, Z.; Juranic, N.; Vikić-Topić, D.; Macura, S. *J. Chem. Inf. Comput. Sci.* **2000**, *40*, 611–621.

(52) Anslyn, E. V.; Dougherty, D. A. In *Modern Physical Organic Chemistry*; University Science Books: Sausalito, California, 2006; p 389.

(53) Cram, D. J.; Choi, H. J.; Bryant, J. A.; Knobler, C. B. *J. Am. Chem. Soc.* **1992**, *114*, 7748–7765.

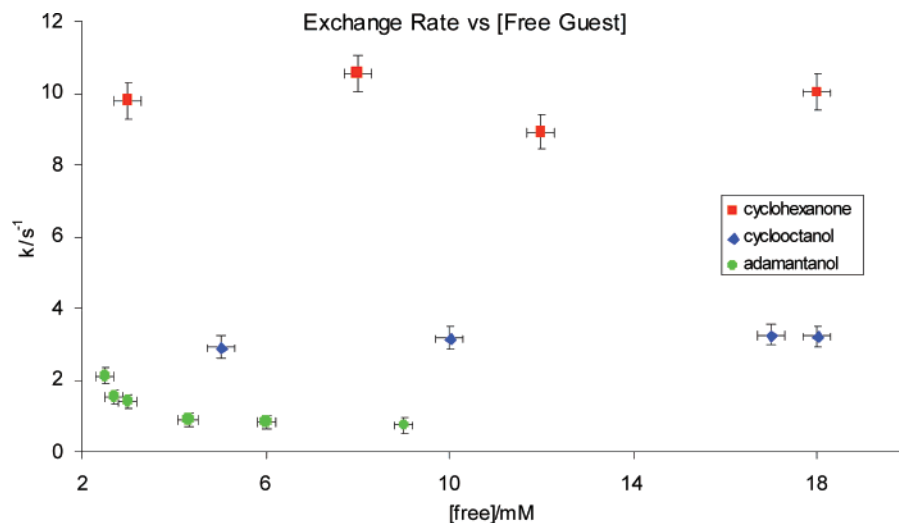


Figure 12. Plot of the concentration dependence of self-exchange of hydrophobic guests in cavitand **1** (2 mM, D₂O).

Co., St. Louis, MO, and were used as received. Molecular modeling (molecular mechanics calculations) was carried out using the AMBER force field²⁶ with the solvation (dielectric) setting for water as implemented by MacroModel or Maestro (Schroedinger, Inc.) on a Silicon Graphics Octane workstation. Cavitand **1** and precursors were synthesized according to the literature procedure.²⁰

8.2. ITC Studies. ITC data were obtained on a VP-ITC MicroCalorimeter, MicroCal, LLC (Northampton, MA). Titrations were performed at 25 °C with a host concentration of approximately 0.1 mM in the cell (1.4348 mL), and a guest concentration of approximately 1 mM in the syringe (250 μL). All solutions were prepared with distilled water. Injection volumes varied from 5 to 10 μL, with a 300-s spacing between injections. All titrations were performed in triplicate. After the reference titration was subtracted, the revised data were fitted to a theoretical titration curve using the One Set of Sites model of the Origin 7.0 software provided by MicroCal, LLC.

8.3. Experimental Procedures. 8.3.a. Synthesis of Dimeric Cavitand 1·1. The cavitand tetraethylester²⁰ (102 mg, 0.073 mmol) was dissolved in a mixture of EtOH (9 mL) and water (6 mL), and NaOH (96 mg, 2.4 mmol) was added as a solid. The mixture was stirred for 30 min, during which time a fine precipitate formed. Additional water (1 mL) gave a clear solution, and stirring was continued at 23 °C for 2 d. The EtOH was slowly removed from the solution by rotary evaporation until a precipitate formed. The mixture was transferred to a centrifuge tube and centrifuged for 20 min. The pellet was retrieved from the supernatant and dried under high vacuum to give the product as an off-white solid (74 mg, 74%). The low solubility of the dimeric complex of **1** in D₂O precluded acquisition of ¹³C NMR spectra in any reasonable amount of time. ¹H NMR (600 MHz, D₂O): δ 0.71 (t, *J* = 7.2 Hz, 24H); 1.85–2.0 (m, 16H); 3.83 (d, *J* = 16.8 Hz, 8H); 3.87 (d, *J* = 16.8 Hz, 8H); 3.97 (dd, *J* = 10.2 Hz, 5.4 Hz, 8H); 6.35 (s, 2H); 6.72 (s, 4H); 6.79 (s, 4H); 6.85 (s, 2H); 7.12 (s, 2H); 7.31 (s, 2H) ESIHRMS (acidic matrix) *m/z*: calcd for C₁₄₄H₁₁₃N₁₆O₃₂ (M + H⁺ of fully protonated tetraacid cavitand dimer) 2577.7701; found 2577.7739.

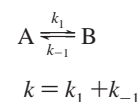
8.3.b. Representative Procedure for Preparation of Host:Gaseous Guest Complexes: Preparation of 1·*n*-Propane. A 2 mM solution of cavitand **1** was formed by mild sonication of **1** (1.7 mg, 0.0012 mmol) in D₂O (0.6 mL) for 5 min. Propane gas was bubbled into the solution slowly to avoid excess foaming for 10 s. The mixture was transferred by pipet to a 5-mm NMR tube for analysis.

8.3.c. Representative Procedure for Preparation of Host:Liquid Guest Complexes: Preparation of 1·*n*-Hexane. A 2 mM solution of cavitand **1** was formed by mild sonication of **1** (1.7 mg, 0.0012 mmol) in D₂O (0.6 mL) for 5 min. *n*-Hexane (5 μL) was added neat, and the

mixture sonicated for 10 min. The mixture was transferred by pipet to a 5-mm NMR tube for analysis.

8.3.d. Representative Procedure for Preparation of Host:Liquid Guest Complexes: Preparation of 1·*n*-Pyrene. A 2 mM solution of cavitand **1** was formed by mild sonication of **1** (1.7 mg, 0.0012 mmol) in D₂O (0.6 mL) for 5 min. Solid pyrene (1 mg) was added, and the resulting suspension sonicated for 24 h. The mixture was microfiltered to remove unextracted solid and transferred by pipet to a 5-mm NMR tube for analysis.

8.4. NMR Studies. 8.4.a. Procedure for 2D NOESY and EXSY Experiments. The 2D NOESY spectra of the cavitands were recorded at 300 K at 600 MHz with the phase-sensitive NOESY pulse sequence supplied with the Bruker software. Each of the 512 F1 increments was the accumulation of 32 scans. Two-dimensional ROESY spectra were also taken to determine whether the cross-peaks observed derived from NOE enhancements or chemical exchange, and were recorded at 300 K at 600 MHz with the phase-sensitive ROESY pulse sequence supplied with the Bruker software. Before Fourier transformation, the FIDs were multiplied by a 90° sine square function in both the F2 and the F1 domain. 1K _ 1K real data points were used, with a resolution of 1 Hz/point. All ROESY spectra were consistent with the NOESY data, but the NOESY spectra are shown here due to the greater resolution and signal-to-noise ratio obtained. For EXSY, two NOESY spectra were taken sequentially, one with 300 ms mixing time and then with 0 ms mixing time. The rate constant *k* was calculated using the EXSYCALC program (Mestrelab Research, Santiago de Compostela)^{50,51} and is the sum of the two dependent magnetization-transfer rate constants obtained from the calculations, an approximation due to the system being in equilibrium.^{46,50,52}



8.4.b. Procedure for DOSY Experiments. The DOSY spectra were acquired using an LED pulse sequence with bipolar gradient pulses and two spoil gradients, as supplied with the Bruker software.⁵⁴ Sine-shaped pulsed gradients were incremented from 2.7 to 51.4 G cm⁻¹ in 32 steps, with each step consisting of 256 scans. The raw data were processed using the MestreC program (Mestrelab Research, Santiago de Compostela).

Acknowledgment. We are grateful to the Skaggs Institute and the National Institutes of Health (GM 50174) for finan-

(54) Wu, D. H.; Chen, A. D.; Johnson, C. S. *J. Magn. Reson., Ser. A* **1995**, *115*, 260–264.

cialsupport. R.J.H. is a Skaggs Postdoctoral fellow. We thank Dr. Laura Pasternack and Dr. Dee-Hua Huang for NMR assistance, and Dr. Shannon Biros for helpful discussions.

Supporting Information Available: ^1H NMR spectra discussed but not present in the text, full predictions of NMR

spectra of bound alkanes, 2D NOESY spectra, raw ITC data. This material is available free of charge via the Internet at <http://pubs.acs.org>.

JA0727058